

ARIS-RSMA Enhanced ISAC System: Joint Rate Splitting and Beamforming Design

Xin Jin, Tiejun Lv, *Senior Member, IEEE*, Yashuai Cao, Jie Zeng, *Senior Member, IEEE*,
and Mugen Peng, *Fellow, IEEE*

Abstract—This letter proposes an active reconfigurable intelligent surface (ARIS) assisted rate-splitting multiple access (RSMA) integrated sensing and communication (ISAC) system to overcome the fairness bottleneck in multi-target sensing under obstructed line-of-sight environments. Beamforming at the transceiver and ARIS, along with rate splitting, are optimized to maximize the minimum multi-target echo signal-to-interference-plus-noise ratio under multi-user rate and power constraints. The intricate non-convex problem is decoupled into three subproblems and solved iteratively by majorization-minimization (MM) and sequential rank-one constraint relaxation (SROCR) algorithms. Simulations show our scheme outperforms non-orthogonal multiple access, space-division multiple access, and passive RIS baselines, approaching sensing-only upper bounds.

Index Terms—Integrated sensing and communication (ISAC), active reconfigurable intelligent surface (ARIS), rate-splitting multiple access (RSMA), multi-target.

I. INTRODUCTION

INTEGRATED sensing and communication (ISAC) signifies a paradigm shift by integrating communication and sensing functions within a unified platform to enhance hardware and spectrum efficiency [1]. However, practical ISAC deployments remain challenged by obstructed line-of-sight (LoS) coverage limitations, intricate interference management, and the fairness bottleneck in sensing multiple targets.

To address the coverage issue, active reconfigurable intelligent surface (ARIS) has been employed to amplify weak incident signals [2]. Current studies on ARIS-ISAC typically optimize beamforming for sensing signal-to-interference-plus-noise ratio (SINR) maximization [3] or energy efficiency optimization [4], primarily under single-target scenarios based on the space-division multiple access (SDMA) scheme. While ARIS enhances link budget, the interference nulling strategy inherent to SDMA results in sub-optimal spatial resource utilization. This inefficiency prevents the system from achieving balanced echo SINR across multiple targets, leading to a critical fairness bottleneck for sensing.

Rate-splitting multiple access (RSMA), which treats part of the interference as a decodable stream, provides a more

Manuscript received 27 December 2025; accepted 5 February 2026. This paper was supported by the National Natural Science Foundation of China under No. 62271068. (corresponding author: Tiejun Lv.)

X. Jin, T. Lv and M. Peng are with the School of Communication and Information Engineering, Beijing University of Posts and Telecommunications, Beijing 100876, China (e-mail: {jxze, lvtiejun, pmg}@bupt.edu.cn).

Y. Cao is with the School of Intelligence Science and Technology, University of Science and Technology Beijing, Beijing 100083, China (e-mail: caoys@ustb.edu.cn).

Jie Zeng is with the School of Cyberspace Science and Technology, Beijing Institute of Technology, Beijing 100081, China (e-mail: zengjie@bit.edu.cn).

flexible and robust interference management strategy [5]. RSMA-based ISAC designs have been shown to improve the communication-sensing trade-off [6], and to enhance multi-user fairness compared to SDMA [7]. Furthermore, RSMA has been combined with transmissive metasurfaces to enable secure ISAC networks [8]. However, these studies typically assume favorable propagation conditions. In LoS-obstructed environments, advanced interference management alone cannot overcome the physical coverage deficit. Recently, ARIS-assisted RSMA-ISAC frameworks have been explored for security-oriented designs under eavesdropper spatial uncertainty [9] and power transfer [10]. While these studies demonstrate the mutual benefits of ARIS and RSMA, the critical problem of fairness-guaranteed multi-target sensing under blockage has yet to be explored.

To bridge this gap, we propose an integrated ARIS-RSMA ISAC framework to circumvent the resource competition bottleneck between multi-user communication and multi-target sensing. Specifically, we leverage RSMA to bypass the resource-intensive nulling requirements of SDMA, effectively harnessing spatial resources for fair multi-target sensing. However, this integration introduces challenges, including the intricate coupling between the ARIS amplification budget and the RSMA stream design, the cascaded non-convexity from the round-trip ARIS structure, and the dual impact of amplified noise on both communication reliability and echo quality.

In this letter, we jointly design the base station (BS) transmit and receive beamformers, ARIS reflection coefficients, and rate-splitting strategy to maximize the minimum multi-target echo SINR under multi-user quality of service (QoS) and power constraints. To resolve this highly coupled problem, a structured block coordinate descent (BCD)-based algorithm is developed. Numerical results validate the superiority of the proposed method over the non-orthogonal multiple access (NOMA), SDMA, and passive RIS (PRIS) baselines, with performance approaching the sensing-only upper bounds.

II. SYSTEM MODEL AND PROBLEM STATEMENT

As shown in Fig. 1, we consider an ARIS-RSMA enhanced ISAC system. The monostatic ISAC BS configured with M transmit/receive antennas simultaneously performs U single-antenna user downlink communication tasks, $\mathcal{U} = \{1, \dots, U\}$, and Q target sensing tasks, $\mathcal{Q} = \{1, \dots, Q\}$. Given that target detection strongly relies on the LoS link between BS and targets, an L -element ARIS, $\mathcal{L} = \{1, \dots, L\}$, is deployed in the ISAC system with blocked targets to enhance sensing and

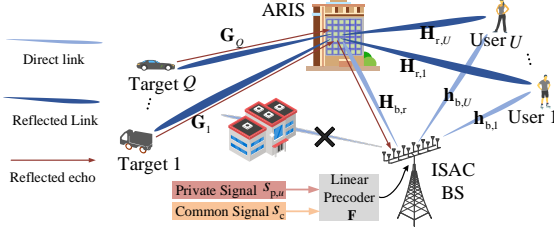


Fig. 1. Illustration of the ARIS-RSMA ISAC system.

communication performance. Define the reflection coefficient of the l -th ARIS element as $\varphi_l = a_l e^{i\theta_l}$, where a_l is the amplification and θ_l is the phase shift. The ARIS beamforming vector is then given by $\varphi = [\varphi_1, \dots, \varphi_L]^T$.

In the RSMA-assisted ISAC system, the transmit data streams comprise private streams for U users, $s_{p,u}, u \in \mathcal{U}$, and a common stream s_c . The message-splitting strategy for private and common streams in RSMA is similar to [6]. Denoting the compound data streams $\mathbf{s} = [s_{p,1}, \dots, s_{p,U}, s_c]^T \in \mathbb{C}^{U+1}$, with $\mathbb{E}(\mathbf{s}\mathbf{s}^H) = \mathbf{I}_{U+1}$, the transmit signal is given by

$$\mathbf{x} = \mathbf{F}\mathbf{s} = \sum_{u \in \mathcal{U}} \mathbf{f}_{p,u} s_{p,u} + \mathbf{f}_c s_c, \quad (1)$$

where $\mathbf{F} = [\mathbf{f}_{p,1}, \dots, \mathbf{f}_{p,U}, \mathbf{f}_c] \in \mathbb{C}^{M \times (U+1)}$. Each column of \mathbf{F} corresponds to the transmit beamforming vector of \mathbf{s} .

Let $\mathbf{H}_{b,r} \in \mathbb{C}^{L \times M}$, $\mathbf{h}_{r,u} \in \mathbb{C}^L$, and $\mathbf{h}_{b,u} \in \mathbb{C}^M$ denote the channel between BS and ARIS, ARIS and user u , BS and user u , respectively. The received signal y_u at user u is given as

$$y_u = (\mathbf{h}_{b,u}^H + \mathbf{h}_{r,u}^H \Phi \mathbf{H}_{b,r}) \mathbf{x} + \mathbf{h}_{r,u}^H \Phi \mathbf{z}_1 + n_u, \quad (2)$$

with $\Phi = \text{diag}(\varphi)$. $\mathbf{z}_1 \sim \mathcal{CN}(\mathbf{0}, \sigma_z^2 \mathbf{I}_L)$ and $n_u \sim \mathcal{CN}(0, \sigma_u^2)$ are the dynamic noise at ARIS and the additive white Gaussian noise (AWGN) at user u , respectively. For simplicity, we define $\mathbf{h}_u^H = \mathbf{h}_{b,r}^H + \mathbf{h}_{r,u}^H \Phi \mathbf{H}_{b,r}$ as the equivalent channel between the BS and user u .

Each user first extracts the common stream s_c from y_u by treating all private streams as interference [6]. After removing s_c via successive interference cancellation (SIC), user u decodes $s_{p,u}$ with the remaining private streams treated as interference. Hence, the SINR of decoding s_c and $s_{p,u}$ at user u are expressed as

$$\gamma_{c,u} = |\mathbf{h}_u^H \mathbf{f}_c|^2 / \left(\sum_{k \in \mathcal{U}} |\mathbf{h}_u^H \mathbf{f}_{p,k}|^2 + \sigma_z^2 \|\mathbf{h}_{r,u}^H \Phi\|^2 + \sigma_u^2 \right), \quad (3)$$

$$\gamma_{p,u} = |\mathbf{h}_u^H \mathbf{f}_{p,u}|^2 / \left(\sum_{k \in \mathcal{U}} |\mathbf{h}_u^H \mathbf{f}_{p,k}|^2 + \sigma_z^2 \|\mathbf{h}_{r,u}^H \Phi\|^2 + \sigma_u^2 \right), \quad (4)$$

with $\tilde{\mathcal{U}} = \mathcal{U} \setminus u$. The corresponding achievable rates are given by $r_{c,u} = \log_2(1 + \gamma_{c,u})$ and $r_{p,u} = \log_2(1 + \gamma_{p,u})$, respectively.

As the targets are blocked, ISAC BS senses Q targets through ARIS-assisted equivalent LoS paths. Thus, the echo signal undergoing the BS-ARIS-target-ARIS-BS path is

$$\mathbf{y}_r = \mathbf{H}_{b,r}^H \Phi^H (\sum_{q \in \mathcal{Q}} \mathbf{G}_q \Phi (\mathbf{H}_{b,r} \mathbf{x} + \mathbf{z}_1) + \mathbf{z}_2) + \mathbf{n}_r, \quad (5)$$

where $\mathbf{G}_q = \beta_q \mathbf{a}(\phi_q) \mathbf{a}^H(\phi_q)$ is the target response matrix between ARIS and target q . β_q is the channel gain coefficient containing path loss and radar cross section (RCS), and $\mathbf{a}(\phi_q) = [1, e^{i\pi \sin \phi_q}, \dots, e^{i(L-1)\pi \sin \phi_q}]^T$ is the array steering vector of ARIS concerning the target direction $\phi_q, q \in \mathcal{Q}$.

$\mathbf{z}_2 \sim \mathcal{CN}(\mathbf{0}, \sigma_z^2 \mathbf{I}_L)$ and $\mathbf{n}_r \sim \mathcal{CN}(\mathbf{0}, \sigma_r^2 \mathbf{I}_M)$ represent the dynamic noise at ARIS and the AWGN, respectively.

Multi-target detection and parameter estimation based on RIS is achievable; hence, we assume that all channels are perfectly known [3]. To ensure reliable detection in obstructed multi-target scenarios, we adopt the max-min echo SINR criterion. This criterion directly couples with detection probability, offers superior tractability for joint beamforming optimization compared to the Cramér-Rao bound (CRB), and provides worst-case performance guarantees [4]. A receive beamformer, $\mathbf{w}_q \in \mathbb{C}^M$, is employed to enhance the echo SINR $\gamma_{r,q}$ of target q , thus $\gamma_{r,q}$ can be written as

$$\begin{aligned} \gamma_{r,q} &= \frac{|\mathbf{w}_q^H \mathbf{H}_{b,q} \mathbf{F} \mathbf{s}|^2}{|\mathbf{w}_q^H \tilde{\mathbf{H}}_{b,q} \mathbf{F} \mathbf{s}|^2 + |\mathbf{w}_q^H (\mathbf{H}_{z_1} \mathbf{z}_1 + \mathbf{H}_{z_2} \mathbf{z}_2 + \mathbf{n}_r)|^2} \\ &= \frac{\mathbf{w}_q^H \mathbf{H}_{b,q} \mathbf{F} \mathbf{F}^H \mathbf{H}_{b,q}^H \mathbf{w}_q}{\mathbf{w}_q^H (\tilde{\mathbf{H}}_{b,q} \mathbf{F} \mathbf{F}^H \tilde{\mathbf{H}}_{b,q}^H + \mathbf{C}) \mathbf{w}_q}, \end{aligned} \quad (6)$$

where $\mathbf{H}_{b,q} = \mathbf{H}_{b,r}^H \Phi^H \mathbf{G}_q \Phi \mathbf{H}_{b,r}$, $\tilde{\mathbf{H}}_{b,q} = \mathbf{H}_{b,r}^H \Phi^H \mathbf{G}_{\tilde{q}} \Phi \mathbf{H}_{b,r}$ with $\mathbf{G}_{\tilde{q}} = \sum_{j \in \mathcal{Q}, j \neq q} \mathbf{G}_j$, $\mathbf{G} = \sum_{q \in \mathcal{Q}} \mathbf{G}_q$, $\mathbf{H}_{z_1} = \mathbf{H}_{b,r}^H \Phi^H \mathbf{G} \Phi$, $\mathbf{H}_{z_2} = \mathbf{H}_{b,r}^H \Phi^H$, and $\mathbf{C} = \sigma_z^2 \mathbf{H}_{z_1} \mathbf{H}_{z_1}^H + \sigma_z^2 \mathbf{H}_{z_2} \mathbf{H}_{z_2}^H + \sigma_r^2 \mathbf{I}_M$.

Our goal is to maximize the worst-case echo SINR over all targets by jointly designing the receive beamformers $\{\mathbf{w}_q\}$, the BS transmit beamformer \mathbf{F} , the ARIS reflection matrix Φ , and the RSMA common rate allocation $\mathbf{c} = [c_1, \dots, c_U]^T \in \mathbb{R}_+^U$, under user's QoS and system power constraints, i.e.,

$$P_0 : \max_{\{\mathbf{w}_q\}, \mathbf{F}, \Phi, \mathbf{c}} \min_{q \in \mathcal{Q}} \gamma_{r,q} \quad (7a)$$

$$\text{s.t. } c_u + r_{p,u} \geq R_u^{\min}, \forall u \in \mathcal{U}, \quad (7b)$$

$$\sum_{k \in \mathcal{U}} c_k \leq r_{c,u}, \forall u \in \mathcal{U}, \quad (7c)$$

$$\|\mathbf{F}\|_F^2 \leq P_{\text{BS}}^{\max} \quad (7d)$$

$$P_{\text{RIS}} \leq P_{\text{RIS}}^{\max}, \quad (7e)$$

$$a_l \leq a_{\max}, \forall l \in \mathcal{L}. \quad (7f)$$

The vector \mathbf{c} is jointly optimized with the beamformers in problem P_0 under the per-user QoS constraint (7b) and the common-stream decodability constraint (7c). This ensures user fairness at a prescribed threshold level, while the remaining spatial degrees of freedom are steered to maximize the minimum echo SINR, thereby enhancing sensing fairness. P_{BS}^{\max} and P_{RIS}^{\max} specify the maximum power budget for ISAC BS and ARIS, respectively. a_{\max} is the maximum amplification factor for each ARIS element. Particularly, P_{RIS} is the reflecting power consumption at ARIS, given by

$$P_{\text{RIS}} = \|\Phi \mathbf{H}_{b,r} \mathbf{F}\|_F^2 + \|\Phi^H \mathbf{G} \Phi \mathbf{H}_{b,r} \mathbf{F}\|_F^2 + \sigma_z^2 \|\Phi^H \mathbf{G} \Phi\|_F^2 + 2\sigma_z^2 \|\Phi\|_F^2. \quad (8)$$

Solving problem P_0 presents critical challenges: i) The fractional forms of the echo SINR in (7a) and the user rate in (7b) and (7c), introduce non-convexity; ii) the quartic objective (7a) and constraint (7e) further increase complexity; and iii) the intricate coupling between the transmit beamforming \mathbf{F} and the reflection coefficient Φ hinders the quest for a global optimal solution of problem P_0 . This motivates the development of a BCD-based iterative algorithm in Section III.

III. ALGORITHM DESIGN

A. Receive Beamforming Design

Considering that the receive beamforming \mathbf{w}_q is only related to the echo SINR in the objective function (7a), we design \mathbf{w}_q by maximizing the echo SINR for target q , written as

$$P_1 : \mathbf{w}_q^{\text{opt}} = \arg \max_{\mathbf{w}_q} \frac{\mathbf{w}_q^H \mathbf{A}_1 \mathbf{w}_q}{\mathbf{w}_q^H \mathbf{A}_2 \mathbf{w}_q}, \forall q \in \mathcal{Q}, \quad (9)$$

where $\mathbf{A}_1 = \mathbf{H}_{b,q} \mathbf{F} \mathbf{F}^H \mathbf{H}_{b,q}^H$, and $\mathbf{A}_2 = \tilde{\mathbf{H}}_{b,q} \mathbf{F} \mathbf{F}^H \tilde{\mathbf{H}}_{b,q}^H + \mathbf{C}$. This problem is a standard generalized Rayleigh quotient optimization problem, thereby the optimal solution $\mathbf{w}_q^{\text{opt}}$ is the eigenvector affiliated with the maximum eigenvalue of $\mathbf{A}_2^{-1} \mathbf{A}_1$. At the t -th iteration, the optimal minimum multi-target SINR after solving the problem P_1 is given by

$$\{\Gamma^{\text{opt}}\}_{P_1}^t = \min_q \frac{(\mathbf{w}_q^{\text{opt}})^H \mathbf{A}_1 \mathbf{w}_q^{\text{opt}}}{(\mathbf{w}_q^{\text{opt}})^H \mathbf{A}_2 \mathbf{w}_q^{\text{opt}}}. \quad (10)$$

B. Joint Transmit Beamforming and Rate-Splitting Design

Given \mathbf{w}_q and Φ , we reformulate the subproblem of jointly optimizing the transmit beamforming \mathbf{F} and rate splitting \mathbf{c} as

$$P_2 : \max_{\mathbf{c}, \{\mathbf{f}_{p,u}\}, \mathbf{f}_c} \min_{q \in \mathcal{Q}} \frac{\sum_{i \in \mathcal{I}} \text{tr}(\mathbf{B}_1 \mathbf{f}_i \mathbf{f}_i^H)}{\sum_{i \in \mathcal{I}} \text{tr}(\mathbf{B}_2 \mathbf{f}_i \mathbf{f}_i^H) + \varepsilon_1} \quad (11a)$$

$$\text{s.t. } \sum_{i \in \mathcal{I}} \text{tr}(\mathbf{f}_i \mathbf{f}_i^H) \leq P_{\text{BS}}^{\max}, \quad (11b)$$

$$\sum_{i \in \mathcal{I}} \text{tr}(\Sigma \mathbf{f}_i \mathbf{f}_i^H) + \varepsilon_2 \leq P_{\text{RIS}}^{\max}, \quad (11c)$$

$$(7b), (7c), \quad (11d)$$

where $\mathcal{I} = \{1, \dots, U, c\}$, and \mathbf{f}_i is the i -th column of \mathbf{F} . $\mathbf{B}_1 = \mathbf{H}_{b,q}^H \mathbf{w}_q \mathbf{w}_q^H \mathbf{H}_{b,q}$, $\mathbf{B}_2 = \tilde{\mathbf{H}}_{b,q}^H \mathbf{w}_q \mathbf{w}_q^H \tilde{\mathbf{H}}_{b,q}$, $\varepsilon_1 = \mathbf{w}_q^H \mathbf{C} \mathbf{w}_q$, $\Sigma = \mathbf{H}_{z_1} \mathbf{H}_{z_1}^H + \mathbf{H}_{z_2} \mathbf{H}_{z_2}^H$, and $\varepsilon_2 = \sigma_z^2 \|\Phi^H \mathbf{G} \Phi\|_F^2 + 2\sigma_z^2 \|\Phi^H\|_F^2$.

Problem P_2 is a non-convex fractional quadratically constrained quadratic programming (QCQP). To handle the quadratic beamforming terms, we lift the vector variables by defining $\mathbf{F}_i = \mathbf{f}_i \mathbf{f}_i^H$, $\forall i \in \mathcal{I}$, and $\mathbf{H}_u = \mathbf{h}_u \mathbf{h}_u^H$, $\forall u \in \mathcal{U}$. The rate constraints (7b) and (7c) are then written as

$$c_u + \log_2(1 + \frac{\text{tr}(\mathbf{H}_u \mathbf{F}_u)}{\sum_{k \in \tilde{\mathcal{U}}} \text{tr}(\mathbf{H}_u \mathbf{F}_k) + \varepsilon_3}) \geq R_u^{\min}, \quad (12)$$

$$\sum_{k \in \mathcal{U}} c_k \leq \log_2(1 + \frac{\text{tr}(\mathbf{H}_u \mathbf{F}_c)}{\sum_{k \in \mathcal{U}} \text{tr}(\mathbf{H}_u \mathbf{F}_k) + \varepsilon_3}). \quad (13)$$

with $\varepsilon_3 = \sigma_z^2 \|\mathbf{h}_{r,u}^H \Phi\|^2 + \sigma_u^2$. Subsequently, we introduce $\{\Gamma\}_{P_x}^t$ as the minimum multi-target SINR when solving problem P_x in the t -th iteration, and reformulate the problem P_2 as

$$\max_{\mathbf{c}, \{\mathbf{F}_i \succeq 0\}, \{\Gamma\}_{P_2}^t} \{\Gamma\}_{P_2}^t \quad (14a)$$

$$\text{s.t. } \sum_{i \in \mathcal{I}} \text{tr}((\mathbf{B}_1 - \{\Gamma\}_{P_2}^t \mathbf{B}_2) \mathbf{F}_i) \geq \{\Gamma\}_{P_2}^t \varepsilon_1, \quad \forall q \in \mathcal{Q}, \quad (14b)$$

$$\sum_{i \in \mathcal{I}} \text{tr}(\mathbf{F}_i) \leq P_{\text{BS}}^{\max}, \quad (14c)$$

$$\sum_{i \in \mathcal{I}} \text{tr}(\Sigma \mathbf{F}_i) \leq P_{\text{RIS}}^{\max} - \varepsilon_2, \quad (14d)$$

$$\text{rank}(\mathbf{F}_i) = 1, \forall i \in \mathcal{I}, \quad (14e)$$

$$(12), (13). \quad (14f)$$

Due to non-convex constraints (14b), (14e), and (14f), this problem remains unsolvable directly. Inspired by the low-complexity SINR approximation algorithm in [11], we resort

to approximate $\{\Gamma\}_{P_2}^t$ on the left-hand side of constraint (14b) based on $\{\Gamma^{\text{opt}}\}_{P_1}^t$ of problem P_1 , i.e.,

$$\sum_{i \in \mathcal{I}} \text{tr}((\mathbf{B}_1 - \{\Gamma^{\text{opt}}\}_{P_1}^t \mathbf{B}_2) \mathbf{F}_i) \geq \{\Gamma\}_{P_2}^t \varepsilon_1, \forall q \in \mathcal{Q}. \quad (15)$$

By introducing a series of non-negative real variables, $\chi = \{\rho_{p,u}, \rho_{c,u}, \xi_{p,u}, \xi_{c,u}\}$, $\forall u \in \mathcal{U}$, and utilizing first-order Taylor approximation techniques, the rate constraints in (14f) are relaxed and approximated by

$$c_u + (\rho_{p,u} - \xi_{p,u})/\ln 2 \geq R_u^{\min}, \quad (16)$$

$$\sum_{k \in \mathcal{U}} \text{tr}(\mathbf{H}_u \mathbf{F}_k) + \varepsilon_3 \geq e^{\rho_{p,u}}, \quad (17)$$

$$\sum_{k \in \tilde{\mathcal{U}}} \text{tr}(\mathbf{H}_u \mathbf{F}_k) + \varepsilon_3 \leq e^{\xi_{p,u}^{(t-1)}} (\xi_{p,u} - \xi_{p,u}^{(t-1)} + 1), \quad (18)$$

$$\rho_{c,u} - \xi_{c,u} \geq \ln 2 \sum_{k \in \mathcal{U}} c_k, \quad (19)$$

$$\sum_{i \in \mathcal{I}} \text{tr}(\mathbf{H}_u \mathbf{F}_i) + \varepsilon_3 \geq e^{\rho_{c,u}}, \quad (20)$$

$$\sum_{k \in \mathcal{U}} \text{tr}(\mathbf{H}_u \mathbf{F}_k) + \varepsilon_3 \leq e^{\xi_{c,u}^{(t-1)}} (\xi_{c,u} - \xi_{c,u}^{(t-1)} + 1). \quad (21)$$

For the rank-one constraint in (14e), rather than completely removing it, we employ sequential rank-one constraint relaxation (SROCR) to progressively tighten the semidefinite relaxation (SDR) solution [12]. Using a flexible parameter ϖ_i , $\varpi_i \in [0, 1]$, (14e) can be substituted with

$$\mathbf{u}_{\max}^H(\mathbf{F}_i^{(t-1)}) \mathbf{F}_i \mathbf{u}_{\max}(\mathbf{F}_i^{(t-1)}) \geq \varpi_i^{(t-1)} \text{tr}(\mathbf{F}_i), \forall i \in \mathcal{I}, \quad (22)$$

where $\mathbf{u}_{\max}(\cdot)$ is the largest eigenvector. We update $\varpi_i^{(t)} = \min(1, \lambda_{\max}(\mathbf{F}_i^{(t)})/\text{tr}(\mathbf{F}_i^{(t)}) + \delta_i^{(t)})$ with an adaptive step size $\delta_i^{(t)}$. Due to space limitations, specific steps and convergence of the SROCR algorithm can be found in [12].

To this end, the problem P_2 is transformed into

$$\max_{\mathbf{c}, \{\mathbf{F}_i \succeq 0\}, \{\Gamma\}_{P_2}^t, \chi} \{\Gamma\}_{P_2}^t \quad (23a)$$

$$\text{s.t.} (14c), (14d), (15) - (22), \quad (23b)$$

which can be solved by the off-the-shelf toolboxes, e.g., CVX.

C. ARIS Reflection Beamforming Design

With the obtained \mathbf{w}_q , \mathbf{F} , \mathbf{c} , and the auxiliary variable $\{\Gamma\}_{P_3}^t$, the ARIS reflect beamforming subproblem is

$$P_3 : \max_{\Phi, \{\Gamma\}_{P_3}^t} \{\Gamma\}_{P_3}^t \quad (24a)$$

$$\text{s.t. } \gamma_{r,q} \geq \{\Gamma\}_{P_3}^t, \forall q \in \mathcal{Q}, \quad (24b)$$

$$(7b), (7c), (7e), (7f). \quad (24c)$$

The core difficulty in solving problem P_3 is that the echo SINR and the ARIS power constraints contain quartic terms in φ . This stems from the round-trip BS-ARIS-target-ARIS-BS echo, where $\Phi = \text{diag}(\varphi)$ is involved twice.

To make the problem tractable, we define $\tilde{\varphi} = \text{vec}(\varphi \varphi^H)$ to reorganize element-pair interactions and reduce the dominant quartic terms to quadratic forms in $\tilde{\varphi}$. Let $\tilde{\mathbf{F}} = \mathbf{H}_{b,r} \mathbf{F} \mathbf{F}^H \mathbf{H}_{b,r}^H$, $\tilde{\mathbf{W}} = \mathbf{H}_{b,r} \mathbf{w}_q \mathbf{w}_q^H \mathbf{H}_{b,r}^H$. Then, the echo SINR in (6) can be rewritten as

$$\gamma_{r,q} = \frac{\tilde{\mathbf{F}}^H \mathbf{M}_1 \tilde{\varphi}}{\tilde{\varphi}^H (\mathbf{M}_2 + \sigma_z^2 \mathbf{M}_3) \tilde{\varphi} + \sigma_z^2 \varphi^H \mathbf{M}_4 \varphi + \sigma_r^2 \mathbf{w}_q^H \mathbf{w}_q}, \quad (25)$$

where $\mathbf{M}_1 = \bar{\mathbf{G}}_q^H (\bar{\mathbf{F}}^T \otimes \bar{\mathbf{W}}) \bar{\mathbf{G}}_q$, $\mathbf{M}_2 = \bar{\mathbf{G}}_{\bar{q}}^H (\bar{\mathbf{F}}^T \otimes \bar{\mathbf{W}}) \bar{\mathbf{G}}_{\bar{q}}$, $\mathbf{M}_3 = \bar{\mathbf{G}}^H (\mathbf{I}_L \otimes \bar{\mathbf{W}}) \bar{\mathbf{G}}$, $\mathbf{M}_4 = \mathbf{I}_L \odot \bar{\mathbf{W}}$, with $\bar{\mathbf{G}}_q = \text{diag}(\text{vec}(\mathbf{G}_q))$, $\bar{\mathbf{G}}_{\bar{q}} = \text{diag}(\text{vec}(\mathbf{G}_{\bar{q}}))$, $\bar{\mathbf{G}} = \text{diag}(\text{vec}(\mathbf{G}))$.

Similar to the treatment of (14b), we approximate constraint (24b) with $\{\Gamma^{\text{opt}}\}_{P_2}^t$, i.e.,

$$\tilde{\varphi}^H \mathbf{M} \tilde{\varphi} + \{\Gamma^{\text{opt}}\}_{P_2}^t \sigma_z^2 \varphi^H \mathbf{M}_4 \varphi \leq \{\Gamma\}_{P_3}^t \tau_q, \forall q \in \mathcal{Q}, \quad (26)$$

where $\mathbf{M} = \{\Gamma^{\text{opt}}\}_{P_2}^t (\mathbf{M}_2 + \sigma_z^2 \mathbf{M}_3) - \mathbf{M}_1$, $\tau_q = -\sigma_r^2 \mathbf{w}_q^H \mathbf{w}_q$. Recall (8), constraint (7e) can be reorganized as

$$\varphi^H \mathbf{D}_1 \tilde{\varphi} + \varphi^H \mathbf{D}_2 \varphi \leq P_{\text{RIS}}^{\text{max}}, \quad (27)$$

where $\mathbf{D}_1 = \bar{\mathbf{G}}^H (\bar{\mathbf{F}}^T \otimes \mathbf{I}_L) \bar{\mathbf{G}} + \sigma_z^2 \bar{\mathbf{G}}^H \bar{\mathbf{G}}$, $\mathbf{D}_2 = (\mathbf{I}_L \odot \bar{\mathbf{F}}) + 2\sigma_z^2 \mathbf{I}_L$.

Based on *Lemma 1* in [4], we approximate the higher-order terms in (26) by majorization-minimization (MM), i.e.,

$$\tilde{\varphi}^H \mathbf{M} \tilde{\varphi} \leq \lambda_M \tilde{\varphi}^H \tilde{\varphi} + 2\Re\{\tilde{\varphi}^H (\mathbf{M} - \lambda_M \mathbf{I}) \tilde{\varphi}_s\} + \tilde{\varphi}_s^H (\lambda_M \mathbf{I} - \mathbf{M}) \tilde{\varphi}_s, \quad (28)$$

where λ_M is the maximum eigenvalue of \mathbf{M} , and $\tilde{\varphi}_s$ is calculated by obtained $\tilde{\varphi}$ in the $(t-1)$ -th iteration. Given that $a_l \leq a_{\text{max}}$, we have $\tilde{\varphi}^H \tilde{\varphi} \leq L^2 a_{\text{max}}^4$. Let $\text{vec}(\mathbf{P}_1) = \mathbf{p}_1 = (\mathbf{M} - \lambda_M \mathbf{I}) \tilde{\varphi}_s$, we further obtain $2\Re\{\tilde{\varphi}^H \mathbf{p}_1\} = 2\Re\{\tilde{\varphi}^H \mathbf{P}_1^H \varphi\} = \tilde{\varphi}^H (\mathbf{P}_1 + \mathbf{P}_1^H) \varphi$. Therefore, (26) is converted into

$$\varphi^H \bar{\mathbf{Q}}_1 \varphi + \eta_1 \leq \{\Gamma\}_{P_3}^t \tau_q, \forall q \in \mathcal{Q}, \quad (29)$$

with $\bar{\mathbf{Q}}_1 = \mathbf{P}_1 + \mathbf{P}_1^H + \{\Gamma^{\text{opt}}\}_{P_2}^t \sigma_z^2 \mathbf{M}_4$, $\eta_1 = \lambda_M L^2 a_{\text{max}}^4 + \tilde{\varphi}_s^H (\lambda_M \mathbf{I} - \mathbf{M}) \tilde{\varphi}_s$. Similarly, by defining $\text{vec}(\mathbf{P}_2) = \mathbf{p}_2 = (\mathbf{D}_1 - \lambda_{D_1} \mathbf{I}) \tilde{\varphi}_s$ with λ_{D_1} being the maximum eigenvalue of \mathbf{D}_1 , (27) is replaced by

$$\varphi^H \bar{\mathbf{Q}}_2 \varphi + \eta_2 \leq P_{\text{RIS}}^{\text{max}}, \quad (30)$$

where $\bar{\mathbf{Q}}_2 = \mathbf{P}_2 + \mathbf{P}_2^H + \mathbf{D}_2$, $\eta_2 = \lambda_{D_1} L^2 a_{\text{max}}^4 + \tilde{\varphi}_s^H (\lambda_{D_1} \mathbf{I} - \mathbf{D}_1) \tilde{\varphi}_s$.

Next, we address the user rate constraints. Since Φ is diagonal, we have $\Phi \mathbf{H}_{b,r} \mathbf{f}_{p,u} = \text{diag}(\mathbf{H}_{b,r} \mathbf{f}_{p,u}) \varphi = \tilde{\mathbf{H}}_u \varphi$, and $\Phi \mathbf{H}_{b,r} \mathbf{f}_c = \text{diag}(\mathbf{H}_{b,r} \mathbf{f}_c) \varphi = \tilde{\mathbf{H}}_c \varphi$. Therefore, the SINR can be reformulated as a quadratic function of φ , i.e.,

$$\gamma_{x,u} = \frac{\varphi^H \mathbf{E}_{x_1} \varphi + 2\Re(\mathbf{E}_{x_2} \varphi) + \tau_{x_1}}{\varphi^H (\mathbf{E}_{x_3} + \sigma_z^2 \mathbf{E}_{x_4}) \varphi + 2\Re(\mathbf{E}_{x_5} \varphi) + \tau_{x_2}}, x \in \{p/c\}, \quad (31)$$

where $\mathbf{E}_{p_1} = \tilde{\mathbf{H}}_u^H \mathbf{h}_{r,u} \mathbf{h}_{r,u}^H \tilde{\mathbf{H}}_u$, $\mathbf{E}_{p_2} = \mathbf{f}_{p,u}^H \mathbf{h}_{b,u} \mathbf{h}_{b,u}^H \tilde{\mathbf{H}}_u$, $\mathbf{E}_{p_3} = \sum_{k \in \mathcal{U}} \tilde{\mathbf{H}}_k^H \mathbf{h}_{r,u} \mathbf{h}_{r,u}^H \tilde{\mathbf{H}}_k$, $\mathbf{E}_{p_4} = \text{diag}(\mathbf{h}_{r,u})^H \text{diag}(\mathbf{h}_{r,u})$, $\mathbf{E}_{p_5} = \sum_{k \in \mathcal{U}} \mathbf{f}_{p,k}^H \mathbf{h}_{b,u} \mathbf{h}_{r,u}^H \tilde{\mathbf{H}}_k$, $\tau_{p_1} = |\mathbf{h}_{b,u}^H \mathbf{f}_{p,u}|^2$, $\tau_{p_2} = \sum_{k \in \mathcal{U}} |\mathbf{h}_{b,u}^H \mathbf{f}_{p,k}|^2 + \sigma_u^2$. On the other hand, $\mathbf{E}_{c_1} = \tilde{\mathbf{H}}_c^H \mathbf{h}_{r,u} \mathbf{h}_{r,u}^H \tilde{\mathbf{H}}_c$, $\mathbf{E}_{c_2} = \mathbf{f}_c^H \mathbf{h}_{b,u} \mathbf{h}_{r,u}^H \tilde{\mathbf{H}}_c$, $\mathbf{E}_{c_3} = \mathbf{E}_{p_1} + \mathbf{E}_{p_3}$, $\mathbf{E}_{c_4} = \mathbf{E}_{p_4}$, $\mathbf{E}_{c_5} = \mathbf{E}_{p_2} + \mathbf{E}_{p_5}$, $\tau_{c_1} = |\mathbf{h}_{b,u}^H \mathbf{f}_c|^2$, $\tau_{c_2} = \tau_{p_1} + \tau_{p_2}$. With the obtained rate splitting vector \mathbf{c} in problem P_2 , we denote $\delta_{1,u} = 2^{R_u^{\text{min}} - c_u} - 1$ and $\delta_2 = 2^{\sum_{u \in \mathcal{U}} c_u} - 1$. Then, (7b) and (7c) are rewritten as $\gamma_{p,u} \geq \delta_{1,u}$ and $\gamma_{c,u} \geq \delta_2$, respectively.

With these transformations, problem P_3 is cast into a QCQP. By defining $\tilde{\varphi} = [\varphi^T, 1]^T$, and $\tilde{\Phi} = \tilde{\varphi} \tilde{\varphi}^H$, we convert it into SDR form and solve it by the SROCR algorithm, i.e.,

$$\max_{\Phi \succeq 0, \{\Gamma\}_{P_3}^t} \{\Gamma\}_{P_3}^t \quad (32a)$$

$$\text{s.t. } \text{tr}(\mathbf{Q}_1 \tilde{\Phi}) + \eta_1 \leq \{\Gamma\}_{P_3}^t \tau_q, \forall q \in \mathcal{Q}, \quad (32b)$$

$$\text{tr}(\mathbf{Q}_2 \tilde{\Phi}) + \eta_2 \leq P_{\text{RIS}}^{\text{max}}, \quad (32c)$$

$$\text{tr}(\mathbf{Q}_3 \tilde{\Phi}) + \tau_{p_1} \geq \delta_{1,u} (\text{tr}(\mathbf{Q}_4 \tilde{\Phi}) + \tau_{p_2}), \forall u \in \mathcal{U}, \quad (32d)$$

$$\text{tr}(\mathbf{Q}_5 \tilde{\Phi}) + \tau_{c_1} \geq \delta_2 (\text{tr}(\mathbf{Q}_6 \tilde{\Phi}) + \tau_{c_2}), \forall u \in \mathcal{U}, \quad (32e)$$

Algorithm 1 The proposed BCD algorithm

Initialize: $\mathbf{F}^{(0)}$, $\Phi^{(0)}$, $\epsilon = 10^{-3}$, $t = 0$

- 1: **repeat**
- 2: $t = t + 1$
- 3: Update $\mathbf{w}_q^{(t)}$ by (9), and calculate $\{\Gamma^{\text{opt}}\}_{P_1}^{(t)}$.
- 4: Update $\mathbf{F}^{(t)}$ by solving (23a), and calculate $\{\Gamma^{\text{opt}}\}_{P_2}^{(t)}$.
- 5: Update $\Phi^{(t)}$ by solving (32a), and calculate $\{\Gamma^{\text{opt}}\}_{P_3}^{(t)}$.
- 6: **until** $|\{\Gamma^{\text{opt}}\}_{P_3}^{(t)} - \{\Gamma^{\text{opt}}\}_{P_3}^{(t-1)}| / \{\Gamma^{\text{opt}}\}_{P_3}^{(t-1)} \leq \epsilon$

Output: $\mathbf{F}^{(t)}$, $\Phi^{(t)}$

Table I: Simulation parameters

Para.	Value	Para.	Value	Para.	Value
M	16	$\alpha_{b,r}$	2.2	ϕ_q	$\{0^\circ, 45^\circ\}$
L	32	$\alpha_{b,u}$	3.5	$P_{\text{BS}}^{\text{max}}$	40 dBm
U	4	$\alpha_{r,u}$	2.3	$P_{\text{RIS}}^{\text{max}}$	20 dBm
Q	2	$\alpha_{r,q}$	2.2	$\sigma_u^2, \sigma_z^2, \sigma_r^2$	-80 dBm

$$\bar{\Phi}_{l,l} \leq a_{\text{max}}^2, \forall l \in \mathcal{L}, \quad (32f)$$

$$\mathbf{u}_{\text{max}}^H (\bar{\Phi}^{(t-1)}) \bar{\Phi} \mathbf{u}_{\text{max}} (\bar{\Phi}^{(t-1)}) \geq \varpi^{(t-1)} \text{tr}(\bar{\Phi}), \quad (32g)$$

where $\mathbf{Q}_1 = \begin{bmatrix} \bar{\mathbf{Q}}_1 & \mathbf{0} \\ \mathbf{0}^T & 0 \end{bmatrix}$, $\mathbf{Q}_2 = \begin{bmatrix} \bar{\mathbf{Q}}_2 & \mathbf{0} \\ \mathbf{0}^T & 0 \end{bmatrix}$, $\mathbf{Q}_3 = \begin{bmatrix} \mathbf{E}_{p_1} & \mathbf{E}_{p_2}^H \\ \mathbf{E}_{p_2} & 0 \end{bmatrix}$, $\mathbf{Q}_4 = \begin{bmatrix} \mathbf{E}_{p_3} + \sigma_z^2 \mathbf{E}_{p_4} & \mathbf{E}_{p_5}^H \\ \mathbf{E}_{p_5} & 0 \end{bmatrix}$, $\mathbf{Q}_5 = \begin{bmatrix} \mathbf{E}_{c_1} & \mathbf{E}_{c_2}^H \\ \mathbf{E}_{c_2} & 0 \end{bmatrix}$, $\mathbf{Q}_6 = \begin{bmatrix} \mathbf{E}_{c_3} + \sigma_z^2 \mathbf{E}_{c_4} & \mathbf{E}_{c_5}^H \\ \mathbf{E}_{c_5} & 0 \end{bmatrix}$, and $\bar{\Phi}^{(t-1)}$ is the optimal solution obtained in the $(t-1)$ -th iteration.

D. Convergence and Complexity Analysis

Algorithm 1 employs a BCD framework to update \mathbf{w}_q , \mathbf{F} , \mathbf{c} , and Φ . In the \mathbf{F} - and Φ -blocks, the SCA surrogates in (15) and (26) are constructed from the latest feasible Γ , so the previous point is feasible for the surrogates and the achieved SINR is non-decreasing with SROCR tightening, i.e., $\{\Gamma\}_{P_1}^{(t)} \leq \{\Gamma\}_{P_2}^{(t)} \leq \{\Gamma\}_{P_3}^{(t)} \leq \{\Gamma\}_{P_1}^{(t+1)}$. SROCR enforces approximately rank-one solutions in both problem P_2 and P_3 without violating these surrogates. Hence, $\Gamma^{(t)}$ is non-decreasing and bounded, guaranteeing Algorithm 1 converges to a stationary point of the relaxed problem. Initialization uses a power-feasible ARIS matrix, maximum ratio transmission (MRT)-based BS beamformers, and a QoS-feasible $\mathbf{c}^{(0)}$.

The dominant complexity of Algorithm 1 comes from solving the SROCR-based subproblems in (23a) and (32a). Using the worst-case complexity of interior-point SDP solvers [13], the overall complexity scales as $\mathcal{O}(I_3(\mathcal{C}_1 + \mathcal{C}_2))$, where $\mathcal{C}_1 = \mathcal{O}(I_1(\max\{M, 7U + Q + 3\}^4 \sqrt{M} \log(1/\epsilon_1)))$, $\mathcal{C}_2 = \mathcal{O}(I_2(\max\{L + 1, 2U + Q + L + 2\}^4 \sqrt{L + 1} \log(1/\epsilon_2)))$. Here I_3 is the outer BCD iteration number, I_1 and I_2 are the inner SROCR iterations, and ϵ_1, ϵ_2 denote the solution accuracies. Compared with ARIS-SDMA, the extra cost mainly stems from the extra rate-splitting constraints in the RSMA design.

IV. NUMERICAL RESULTS

This section evaluates the proposed ARIS-RSMA-assisted ISAC scheme and the joint design algorithm through numerical simulation. The channel model with large- and small-scale fading is similar to [3], where $\alpha_{b,r}$, $\alpha_{b,u}$, $\alpha_{r,u}$ and $\alpha_{r,q}$

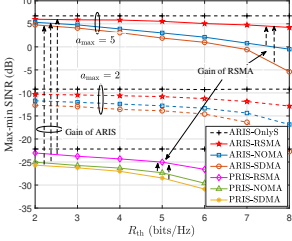
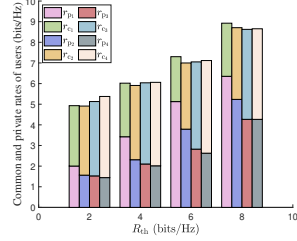
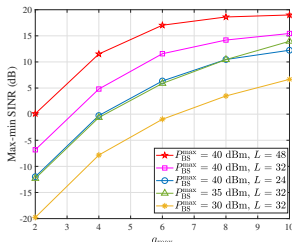
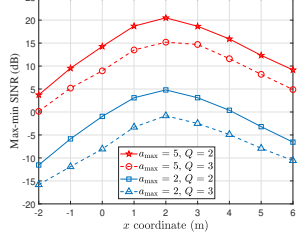
Fig. 2. Max-min SINR vs. R_{th} .Fig. 3. Rate allocation vs. R_{th} .Fig. 4. Max-min SINR vs. a_{max} .

Fig. 5. Max-min SINR vs. ARIS location.

are the path-loss exponents for the BS-RIS, BS-user, RIS-user, and RIS-target channels, respectively. We set $\delta_i^{(0)} = 0.1$ for all SROCR updates. Unless otherwise stated, the specific parameter configurations are listed in Table I. To verify the performance superiority of ARIS and RSMA in ISAC systems (ARIS-RSMA), we also provide comparisons with benchmarks based on PRIS, NOMA, SDMA, and sensing-only schemes (OnlyS).

Fig. 2 shows the max-min multi-target echo SINR versus R_{th} for different schemes. As R_{th} increases, all communication enabled schemes suffer a sensing loss, while ARIS always outperforms PRIS. A larger a_{max} further strengthens the coverage-limited echo link. For a fixed RIS architecture, RSMA yields higher worst-target echo SINR than NOMA and SDMA, e.g., at $R_{th} = 5$ bits/Hz, 5.54, 3.02, 1.91 dB for ARIS-RSMA, ARIS-NOMA, ARIS-SDMA, respectively. This is because SDMAs private-only transmission consumes more spatial resources to meet QoS, NOMAs fixed SIC constraints limit rebalancing under ARIS power and noise coupling, whereas RSMAs common-private structure best exploits the ARIS-enhanced spatial resources for weakest-target protection.

Fig. 3 depicts the common and private rate allocation versus R_{th} for ARIS-RSMA. When R_{th} is small, most user rates are carried by the common stream and only modest private rates are needed, leaving more power and spatial degrees of freedom for sensing. As R_{th} grows, the common rate becomes limited by the weakest user, so the optimizer shifts power to private streams, causing the private-rate share to increase while the common rate saturates and the max-min echo SINR decreases.

Fig. 4 presents the max-min echo SINR versus a_{max} . Given P_{BS}^{\max} and L , increasing a_{max} improves the echo SINR but with diminishing returns, as the ARIS power constraint and amplified noise gradually limit the effective gain. Higher P_{BS}^{\max} or larger L shift the curves upward, indicating that a moderate a_{max} , e.g., 5, is sufficient to harvest most of the ARIS gain

without incurring excessive ARIS power consumption.

Fig. 5 plots the max-min echo SINR versus the ARIS horizontal coordinate x for different target numbers and amplification factors. All curves exhibit a clear peak around $x \approx 2$ m, indicating that the ARIS should be deployed near, but not necessarily closest to, the blocked sensing region to balance the BS-ARIS-target round-trip gain and the ARIS-assisted user links under QoS constraints. Increasing a_{max} from 2 to 5 and reducing the number of targets from $Q = 3$ to $Q = 2$ consistently shift the curves upward, which confirms that stronger amplification and lower target density are conducive to safeguarding the worst-target performance.

V. CONCLUSION

This letter presents an ARIS-RSMA-enhanced ISAC framework to address the fairness challenge in multi-target sensing under obstructed LoS conditions. We formulate a joint optimization problem for beamforming and rate splitting, solved via an efficient BCD algorithm, to guarantee worst-case sensing performance across multiple targets. Simulation results demonstrate that the proposed scheme maintains user QoS while significantly improving sensing robustness and fairness, offering an effective solution for ISAC in complex propagation environments.

REFERENCES

- [1] C. Yang, X. Wang, W. Ni, and Y. Jiang, "Optimal beamforming for MIMO DFRC systems with transmit covariance constraints," *IEEE Trans. Signal Process.*, vol. 73, pp. 601–616, Jan. 2025.
- [2] Z. Yu, H. Ren, C. Pan *et al.*, "Active RIS-aided ISAC systems: Beamforming design and performance analysis," *IEEE Trans. Commun.*, vol. 72, no. 3, pp. 1578–1595, Mar. 2024.
- [3] Q. Zhu, M. Li, R. Liu, and Q. Liu, "Joint transceiver beamforming and reflecting design for active RIS-aided ISAC systems," *IEEE Trans. Veh. Technol.*, vol. 72, no. 7, pp. 9636–9640, Jul. 2023.
- [4] J. Ye, M. Rihan, P. Zhang *et al.*, "Energy efficiency optimization in active reconfigurable intelligent surface-aided integrated sensing and communication systems," *IEEE Trans. Veh. Technol.*, vol. 74, no. 1, pp. 1180–1195, Jan. 2025.
- [5] B. Clerckx, Y. Mao, E. A. Jorswieck *et al.*, "A primer on rate-splitting multiple access: Tutorial, myths, and frequently asked questions," *IEEE J. Sel. Areas Commun.*, vol. 41, no. 5, pp. 1265–1308, May. 2023.
- [6] C. Xu, B. Clerckx, S. Chen *et al.*, "Rate-splitting multiple access for multi-antenna joint radar and communications," *IEEE J. Sel. Topics Signal Process.*, vol. 15, no. 6, pp. 1332–1347, Nov. 2021.
- [7] K. Chen, Y. Mao, L. Yin *et al.*, "Rate-splitting multiple access for simultaneous multi-user communication and multi-target sensing," *IEEE Trans. Veh. Technol.*, vol. 73, no. 9, pp. 13 909–13 914, Sep. 2024.
- [8] Z. Liu, W. Chen, Q. Wu, Z. Li, X. Zhu, Q. Wu, and N. Cheng, "Enhancing robustness and security in ISAC network design: Leveraging transmissive reconfigurable intelligent surface with RSMA," *IEEE Trans. Commun.*, vol. 73, no. 10, pp. 9581–9596, Mar. 2025.
- [9] A. A. Salem, S. Abdallah, M. Saad, K. Alnajjar, and M. A. Albreem, "Robust secure ISAC: How RSMA and active RIS manage eavesdropper's spatial uncertainty," *IEEE Trans. Veh. Technol.*, pp. 1–16, Sep. 2025.
- [10] A. Abdelaziz Salem, K. Alnajjar, M. A. Albreem, M. Saad, and S. Abdallah, "Active RIS enabled RSMA integrated sensing, communication, and power transfer," *IEEE Trans. Commun.*, pp. 1–1, Aug. 2025.
- [11] J. Zhou, H. Li, and W. Cui, "Low-complexity joint transmit and receive beamforming for MIMO radar with multi-targets," *IEEE Signal Process. Lett.*, vol. 27, pp. 1410–1414, Aug. 2020.
- [12] P. Cao, J. Thompson, and H. V. Poor, "A sequential constraint relaxation algorithm for rank-one constrained problems," in *Proc. Eur. Signal Process. Conf. (EUSIPCO)*, Kos, Greece, Aug. 2017, pp. 1060–1064.
- [13] X. Mu, Y. Liu, L. Guo, J. Lin, and N. Al-Dhahir, "Exploiting intelligent reflecting surfaces in NOMA networks: Joint beamforming optimization," *IEEE Trans. Wireless Commun.*, vol. 19, no. 10, pp. 6884–6898, Oct. 2020.